DOING PHYSICS WITH PYTHON

COMPUTATIONAL OPTICS

RAYLEIGH-SOMMERFELD 1 DIFFRACTION INTEGRAL CIRCULAR APERTURE:

FOCUSED BEAM

Ian Cooper

Please email me any corrections, comments, suggestions or additions: **matlabvisualphysics@gmail.com**

DOWNLOAD DIRECTORIES FOR PYTHON CODE

Google drive

GitHub

emRSFBXY.py

Calculation of the radiant flux density (irradiance) in a plane perpendicular to the optical axis for the radiant flux of convergent beam emitted from a circular aperture.

emRSFBZ.py

Calculation of the radiant flux density (irradiance) along the optical axis for the radiant flux of convergent beams emitted from a circular aperture.

emFBZX.py

Calculation of the irradiance in the meridional (XZ plane) for the radiant flux of convergent beam emitted from a circular aperture.

Warning: The results of the integration may look OK but they may not be accurate if you have used insufficient number of partitions for the aperture space and observation space. It is best to check the convergence of the results as the number partitions is increased. Note: as the number of partitions increases, the calculation time **rapidly** increases.

It is necessary to modify the Python Codes and comment or uncomment lines of code to run the simulations with different input and output parameters.

RAYLEIGH-SOMMERFELD DIFFRACTION INTEGRAL OF THE FIRST KIND

The **Rayleigh-Sommerfeld diffraction integral of the first kind** states that the electric field $E_P\left(x_P, y_P, z_P\right)$ at an observation point P $\left(x_P, y_P, z_P\right)$ can be expressed as

$$(1)\quad E_P\left(x_P, y_P, z_P\right) = \frac{1}{2\pi}\iint_{S_A} T\, E_Q\, \frac{e^{j\,k\,r_{PQ}}}{{r_{PQ}}^3} z_p\,(j\,k\,r_{PQ} - 1)\, dx_Q\, dy_Q$$

planar aperture space

where is the electric field within the aperture space is $E_Q\left(x_Q, y_Q, z_Q\right)$ and is r_{PQ} the distance from an observation point P to an aperture point Q$\left(x_Q, y_Q, z_Q\right)$. The term T is a transmission function for a filter to modify the electric field within the pupil or an aberration factor. If there is no mask or zero aberration effects then T = 1

It is assumed that the Rayleigh-Sommerfeld diffraction integral of the first kind is valid throughout the space in front of the aperture, right down to the aperture itself. There are no limitations on the maximum size of either the aperture or observation region, relative to the observation distance, because **no approximations have been made**.

The diffraction pattern in the observation space can be given in terms of the irradiance distribution I_P

(2) $$I_P = \frac{n\varepsilon_0 c}{2} E_P^{*} E_P$$

where ε_0 is the permittivity of free space, c is the speed of light in vacuum, n is the refractive index of the medium.

The time rate of flow of radiant energy is the **radiant flux** W_P where

(3) $$W_P = \iint_{area} I_P \, dA$$

Most physical quantities are expressed in S.I. UNITS

Quantity	**S.I. unit**
distances	m
electric field	$V.m^{-1}$
speed of light	$m.s^{-1}$
permittivity of free space	$C^2.N^{-1}.m^{-2}$
irradiance, radiant flux density	$W.m^{-2}$
time rate of radiance energy, radiant flux	W or $J.s^{-1}$

IMAGE FORMATION AND ITS RELATIONSHIP TO DIFFRACTION

The scalar theory of diffraction can be used to describe the formation of images and to account for the effects of aberrations that distort the image. Knowledge of the irradiance near the focal region is important for the performance of microscopes, telescopes and the focussing of lasers.

In a Gaussian image forming system, light from an object is focused by a lens to form an image of the object. In this geometrical optics approach, light from each point on the object is focused to a point in the image plane. However, due to the finite size of the lens and aberration effects, the light from a point on the object can't be focused to a point in the image plane. The image from each point on the object is smeared out reducing the resolution and degrading the quality of the image of the object.

It is possible to calculate the three-dimensional radiant flux density (irradiance) pattern in the image (observation) space for the light coming from a point source object. This calculation provides details of the smearing out of the image of the point source. This calculation forms part of the Abbey theory of image formation, where the electric field in the image space is found using the Fresnel-Kirchhoff diffraction integral. But many approximations and much algebra are needed to find the

electric field and the results are only applicable to special situations.

A much easier way to calculate the electric field in the image space and without all the algebra and approximations is to simply use the Rayleigh-Sommerfeld diffraction integral of the first kind (RS1) as given in equation (1) and finding the electric field by numerical integration using [2D] Simpson's rule.

Figure 1 shows a simple arrangement for the focusing of a point source by a lens. The image is also just a point. We can discuss the electric field from a single point and then obtain the electric field distribution at the image by a coherent superposition of all the point sources. The object distance d_1, the image distance d_2 and the focal length of the lens *f* are connected by the thin lens equation

$$\frac{1}{d_1}+\frac{1}{d_2}=\frac{1}{f}$$

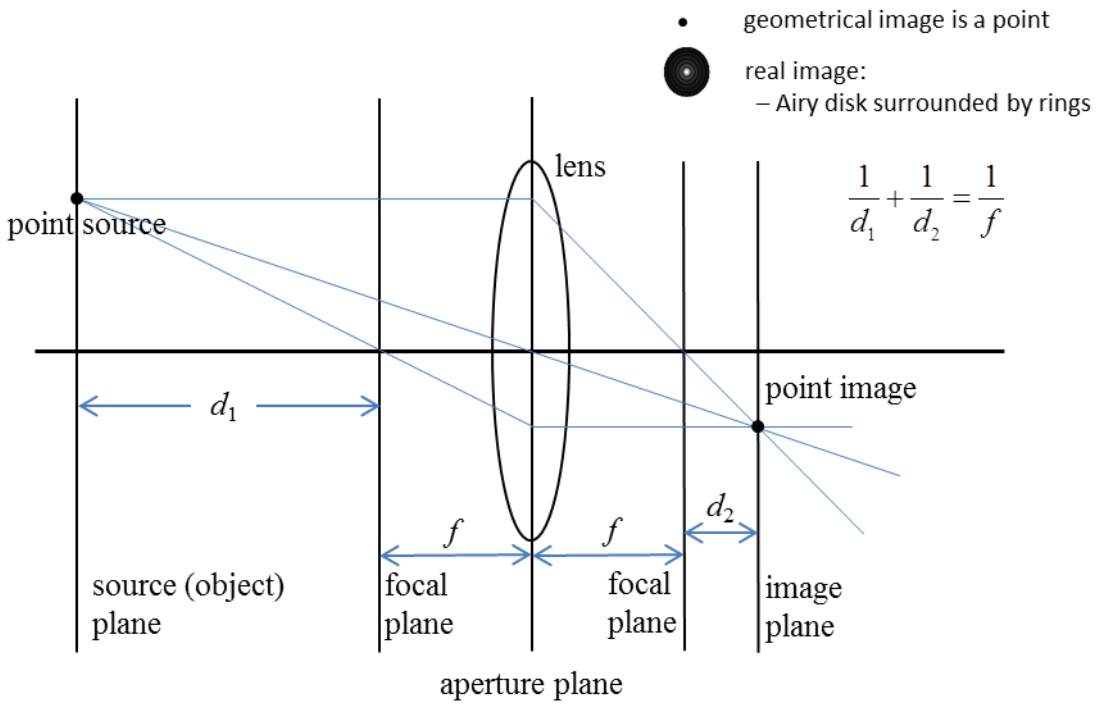

Fig. 1. Gaussian optical system for the focussing action of a lens for a point source.

A focused beam of monochromatic radiation (wavelength λ and propagation constant $k = 2\pi / \lambda$) from a lens is modelled by considering the convergence of spherical waves to the geometrical focus of the lens. If the point source is located at an infinite from the aperture, then the focal plane and image plane coincide and the image is formed in the focal plane.

$$d_1 \to \infty \quad \frac{1}{d_1} \to 0 \quad d_2 \to f$$

For the point source where $d_1 \to \infty$, we replace the focussing action of the lens by considering the convergence of spherical wavefronts from a circular aperture to a focus point at the position of the focal plane. The point source $\mathrm{S}(x_S, y_S, z_S)$ is

now located at the geometrical focus of the converging spherical waves and at a distance r_{OS} from the origin O located at the centre of the aperture as shown in figures 2 and 3.

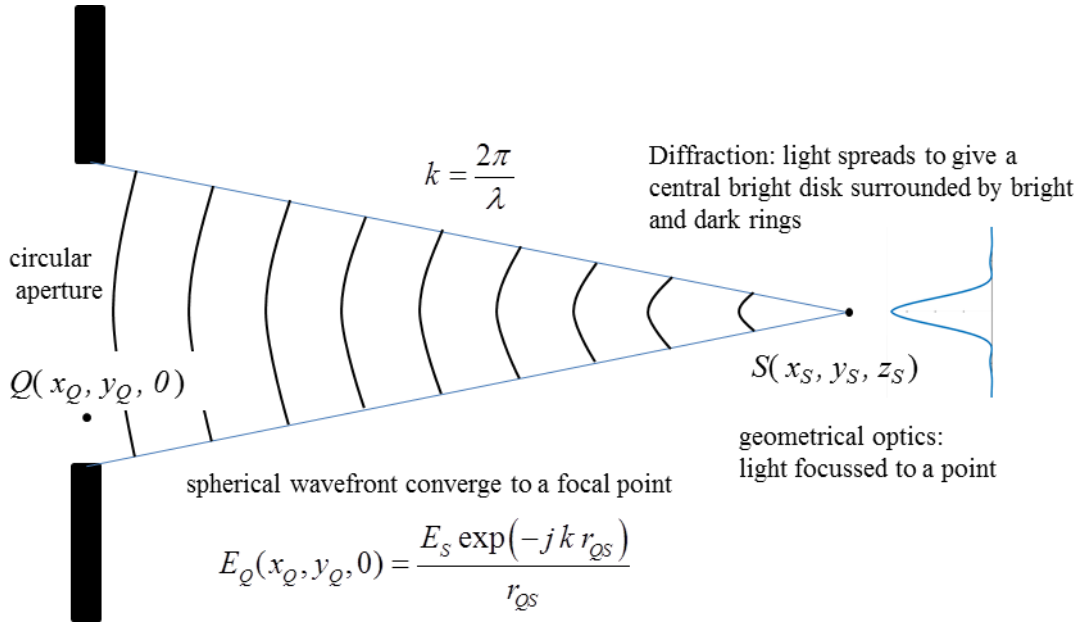

Fig. 2. Spherical waves from a circular aperture converge to a focal point.

The electric field E_Q of strength E_S at an aperture point $Q\left(x_Q, y_Q, z_Q\right)$ at a distance r_{QS} from the source point S $\left(x_S, y_S, z_S\right)$ is given by

$$(4) \quad E_Q(x_Q, y_Q, 0) = \frac{E_S \exp\left(-j k r_{QS}\right)}{r_{QS}}$$

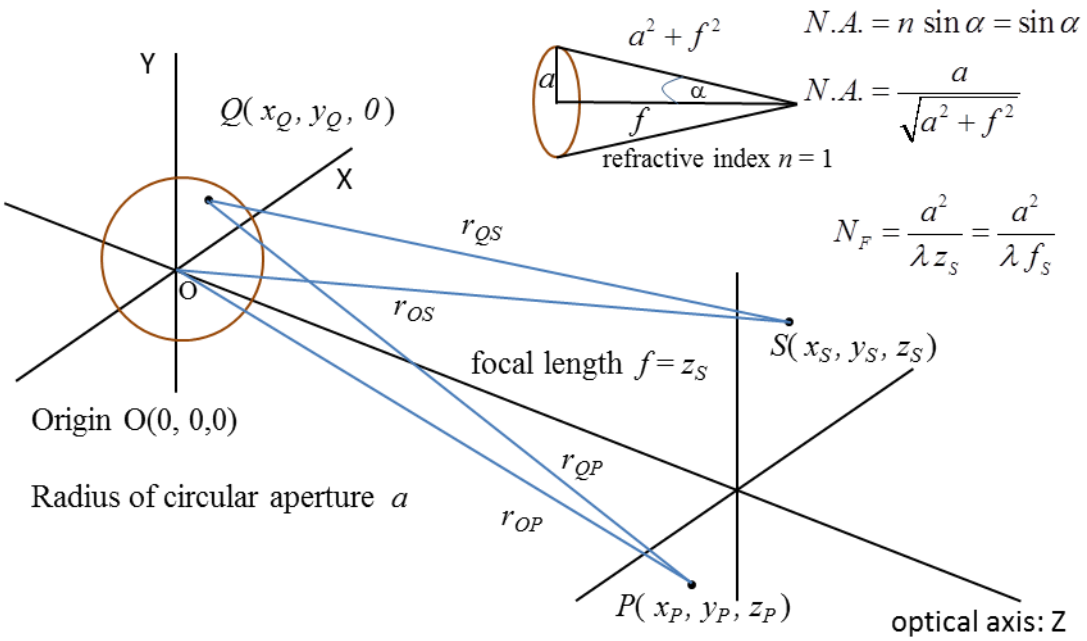

Fig. 3. Geometry for the calculation of E_P for the spherical waves emitted from the circular aperture to the focal point S.

For spherical waves shown in figure 2, the radiant flux would always be confined to a cone and so the radiant flux density would be infinite at the focus point. This can't happen; the energy carried by the wave must spread so the focal point must have some finite size. This phenomenon is called **diffraction**, that is, diffraction results from the limitations of the size of the wave surface emerging through the finite exit pupil of the aperture. Also, aberrations reduce the central radiant flux density with more energy being in the outer rings and the diffraction pattern may no longer be symmetrical about the optical axis, hence, aberrations cause a further spreading of the image of the point source. The total image field plane is a

superposition of all the individual diffraction patterns when the proper accounting is done for the relative phases.

The **numerical aperture** NA of an optical system is a dimensionless number that characterizes the range of angles over which the system can accept or emit light (figure 3). In most areas of optics, and especially in microscopy, the numerical aperture of an optical system such as an objective lens is defined by

(6) $$NA = n \sin\alpha = \frac{n\,a}{\sqrt{a^2 + f^2}}$$

The refractive index is n = 1 will only be considered, and α is the half-aperture angle of the maximum cone of light that can enter or exit the lens. In general, this is the angle of the real marginal ray in the system. Most approximation methods for calculating the irradiance in the focal region assume that the numerical aperture NA is small and the radius of the aperture is much greater than the wavelength

(7) $(NA)^2 << 1$ or $a^2 / f^2 << 1$ and $a >> \lambda$

By the direct numerical integration of diffraction integrals, these limitations are not so restrictive.

The irradiance in the focal region depends upon the wavelength λ, aperture radius a, and the focal distance $f = z_S$. To characterize the focusing geometry, the **Fresnel number** N_F is defined by

(8) $$N_F = \frac{a^2}{\lambda z_S}$$

The Fresnel number can be thought of as the number of Fresnel zones that fill the aperture when the aperture is viewed from the geometrical focus. The wave field near the geometrical focus region depends upon the Fresnel number.

For calculating the irradiance, it is useful to define two optical coordinates for the axial and radial directions

(9) $$u_P = \frac{k\,a^2}{z_S{}^2}\left(z_P - z_S\right)$$ axial optical coordinate

(10) $$v_P = \frac{k\,a}{z_S} x_P$$ radial optical coordinate

For low numerical apertures $(NA)^2 << 1$, the Fresnel number N_F is an excellent parameter in describing the structure of the focal region. Low *NA* focusing system corresponds to the and it can be shown that the axial and radial irradiance distributions are described by simple analytical expressions

(11) $$I(u_P,0) = I_{max}\left(\frac{\sin(u_P/4)}{(u_P/4)}\right)^2$$ axial irradiance

(12) $$I(0,v_P) = I_{max}\left(\frac{2\,J_1(v_P)}{v_P}\right)^2$$ radial irradiance

Equations 11 and 12 can be derived from the Fresnel-Kirchhoff diffraction integral using the **Debye parabolic approximation** where spherical wavefronts are replaced by paraboloids in paraxial systems. Equations 11 and 12 imply that in the neighbourhood of the focal region, the irradiance distribution is symmetrical about the focal plane with the maximum irradiance occurring at the geometrical focus.

The zeros along the optical axis occur at

(13)

$$u_P = 12.57,\ 25.13,\ 37.70,\ 50.27,\ \ldots = 4\pi(1,\ 2,\ 3,\ 4,\ 5,\ \ldots)$$

The irradiance distribution in the focal plane is the familiar Airy disk pattern where J_1 is the Bessel function of the first kind and the zeros in the radial direction occur at

(14) $$v_P = 3.84\ \ 7.02\ \ 10.17\ \ 13.33\ \ 16.47\ \ 19.62\ \ \ldots$$

Equations 11 to 14 describe the Fraunhofer diffraction in the focal region.

Rayleigh-Sommerfeld diffraction integral of the first kind numerical integration using [2D] Simpson's rule

The geometry of the aperture and observation spaces is shown in figure 4, and figure 5 shows an outline of how to the RS1 diffraction integral is computed in Python.

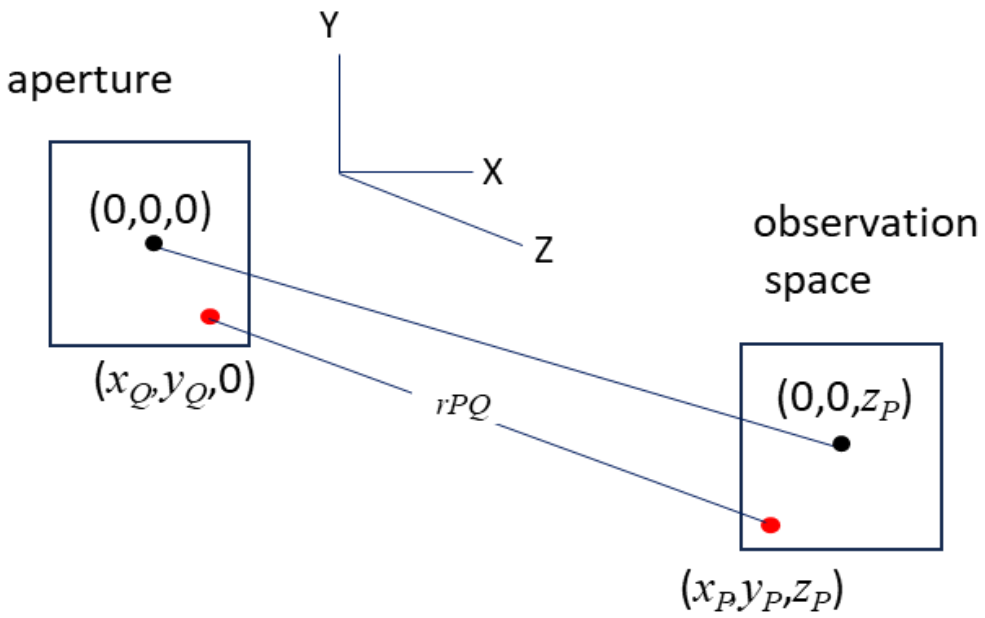

Fig. 4. Geometry of the aperture and observation spaces.

Rayleigh-Sommerfeld 1 diffraction integral

$$E_P = \frac{1}{2\pi}\int_{a_x}^{b_x}\int_{a_y}^{b_y} E_Q \frac{e^{j k r_{PQ}}}{r_{PQ}^{\,3}} z_p \,(j k r_{PQ} - 1)\; dx\, dy$$

numerical integration:
[2D] Simpson's 1/3 rule

$$E_P(x_P, y_P, z_P)$$

$$= \left(\frac{h_x h_y}{9}\right) z_P \sum_{m=1}^{n_Q} \sum_{n=1}^{n_Q} \left(\left(\frac{e^{j k\, r_{PQmn}}}{r_{PQmn}^{\,3}} \right) \left(j k r_{PQmn} - 1\right) \left(E_{Qmn} S_{mn}\right) \right)$$

$$h_x = \frac{b_x - a_x}{n_Q - 1}$$

$$h_y = \frac{b_y - a_y}{n_Q - 1}$$

matrix **MP** $n_Q \times n_Q$

matrix **EQ** $n_Q \times n_Q$

matrix **S** $n_Q \times n_Q$

Fig. 5. Matrices used in computed the diffraction integral.

SIMULATIONS

The irradiance pattern surrounding the focal point depends on the values of the numerical aperture NA and Fresnel number NF. The simulations will consider three examples.

1. Small NA and large NF (Debye approximation / Fraunhoffer diffraction is valid)
2. Large NA and large NF (Debye approximation / Fraunhoffer diffraction is **not** valid)
3. Large NA and small NF (Debye approximation / Fraunhoffer diffraction is **not** valid)

For each simulation, the results are summarized in the Console Window and in Figure Windows. The default wavelength for all simulations is $\lambda = 500 \text{ nm}$ (wL). The computation for the irradiance in the XY and ZX planes may take several minutes.

The irradiance patterns are insensitive to changes in wavelength, aperture radius or focal length when plotted in terms of the optical coordinates v_P and u_P. Therefore, the Fresnel number is an excellent parameter for describing the irradiance in the focal region.

1. Small NA and large NF FRAUNHOFFER DIFFRACTION

focal length f = 0.20 m aperture radius a = 0.010 m

NA = 0.050 *NF* = 1000

Source (0,0, $z_P = f$ = 0.200 m)

Aperture space

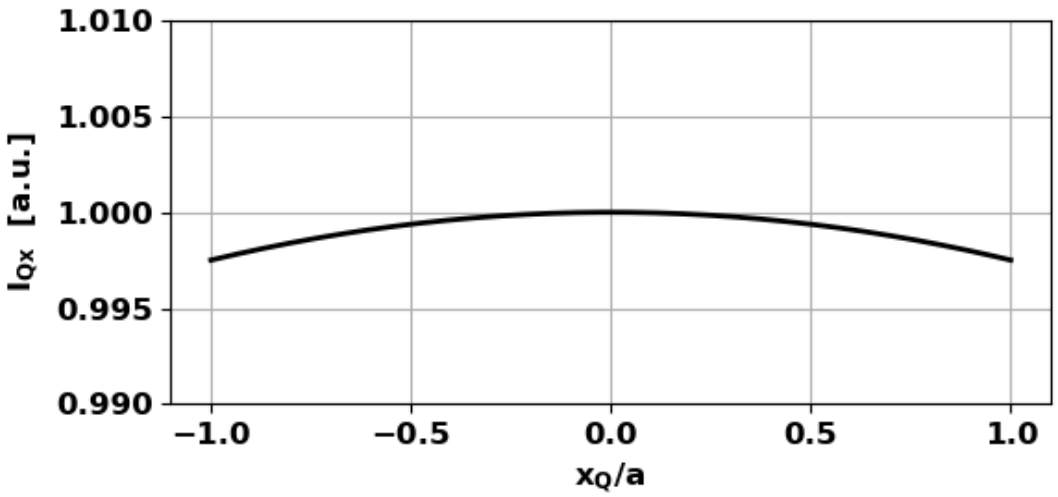

Fig. 6. Aperture space: normalized irradiance distribution along X axis in the plane of the aperture.
$(a = 0.01\ \text{m} \quad z_S = 0.20\ \text{m} \quad NQ = 120)$

Observation space

Irradiance along the optical axis near the focal point

emRSFBZ.py

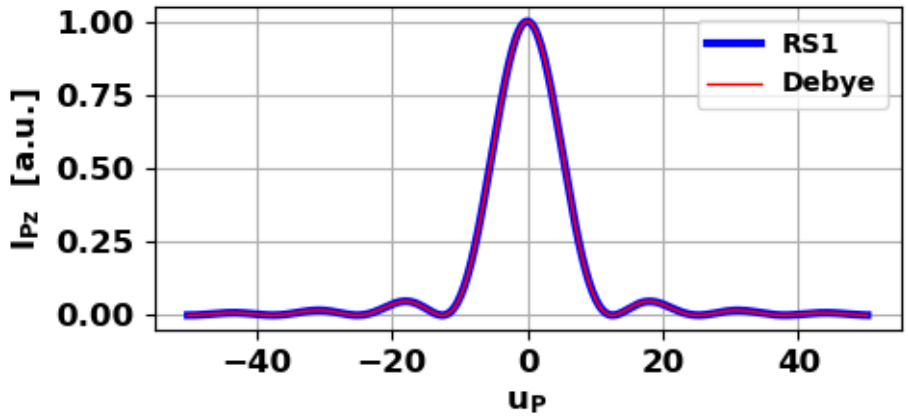

Fig. 7A. Normalized irradiance along the optical axis. Blue curve (RS1) and red curve (Debye).

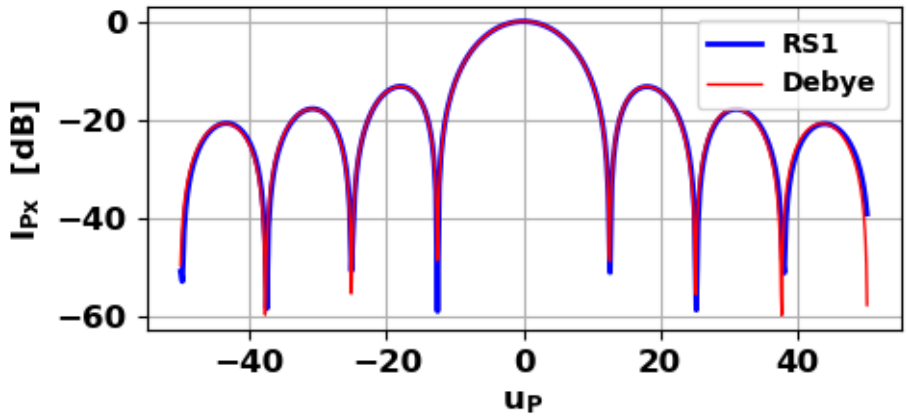

Fig. 7B. Normalized irradiance (dB) along the optical axis. Blue curve (RS1) and red curve (Debye). The zeros (minima) at uP are shown in the Console Window. For small NA and large NF, there is excellent agreement between the irradiance patterns computed by RS1 and the Debye approximation.

Min at uP 12.74 25.14 38.13 50.83

Values agree with equation 13 predictions.

Irradiance in the XY focal plane emRSFBXY.py

Figure 8 shows the excellent agreement between the predictions of the **RS1** calculation and the Debye approximation (equation 12).

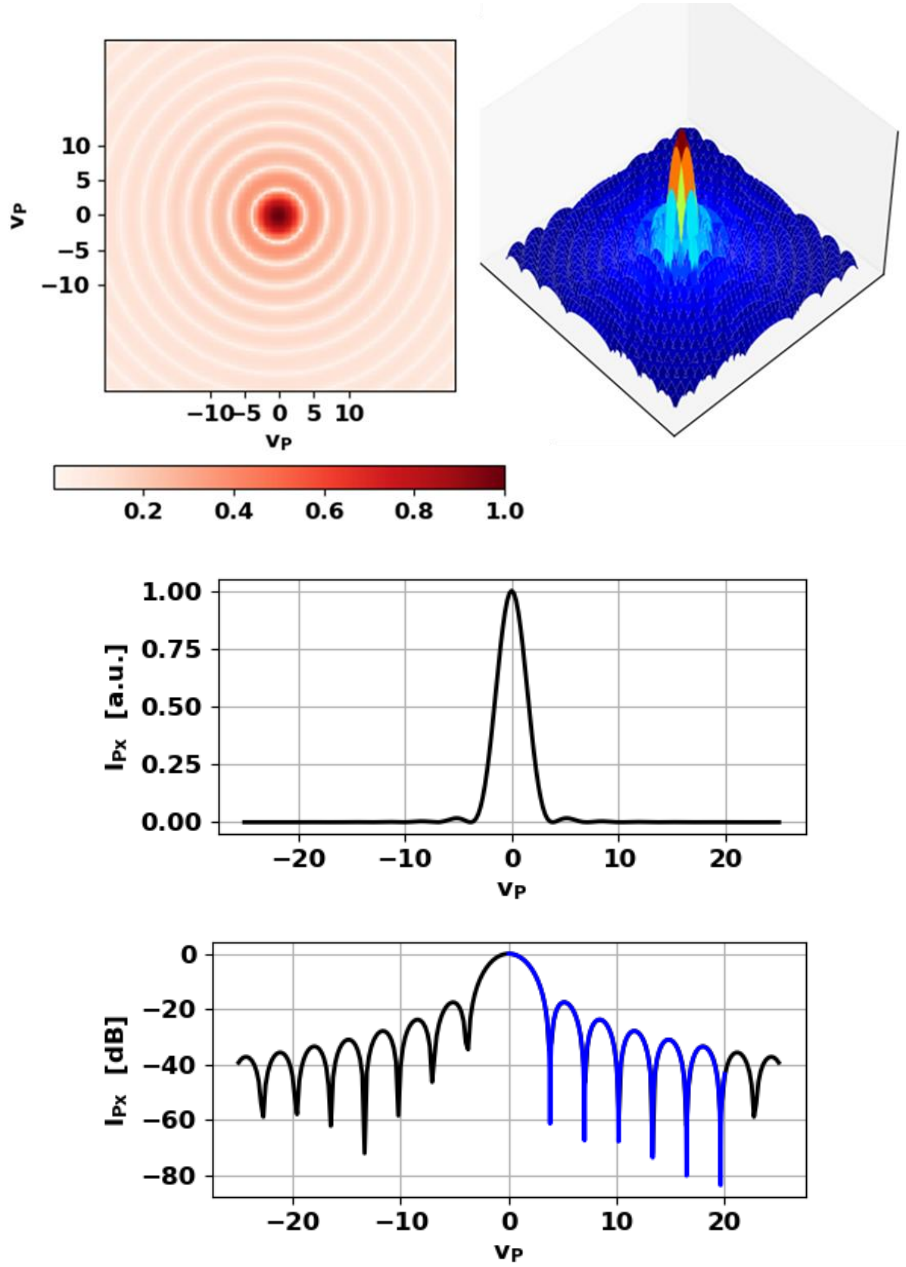

Fig. 8. Normalized irradiance in the focal plane. Blue curve for the Debye approximation

$\left(NP = 120 \quad z_P = 0.20\ m \quad sf = 0.25 \quad I^{sf} \right).$

The Console Window displays radial coordinate values for the zeros in the irradiance distribution for the RS1 and Debye predictions. The values confirm the excellent agreement between the RS1 and Debye approximations.

Dark rings vP *RS1 calculations*

3.77 7.00 10.23 13.46 16.52 19.75

Dark rings Bessel function zeros *equation 12 calculations*

3.84 7.02 10.17 13.33 16.47 19.62

Irradiance in the meridional ZX plane emRSFBZX.py

Figure 9 shows the irradiance distribution in the meridional ZX plane.

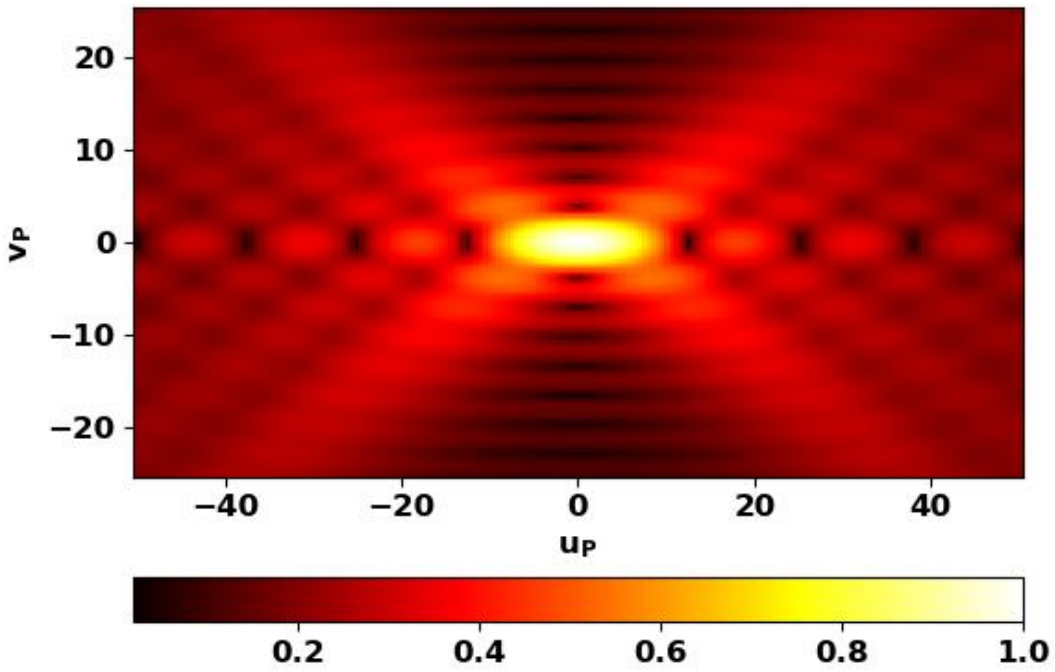

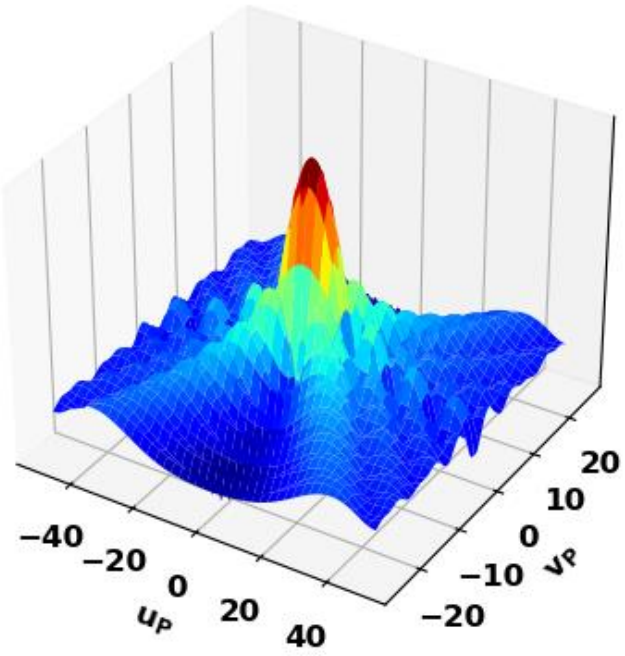

Fig. 9. [2D] and [3D] views of the scaled irradiance distribution in the meridional ZX plane. The [2D] view uses the **pcolormesh** function

```
cf = ax.pcolormesh(UP,VP,IZX**sf, cmap='hot')
fig2.colorbar(cf, ax=ax, location = 'bottom')
```

Figure 10 shows the meridional irradiance pattern using the Python command **contour**.

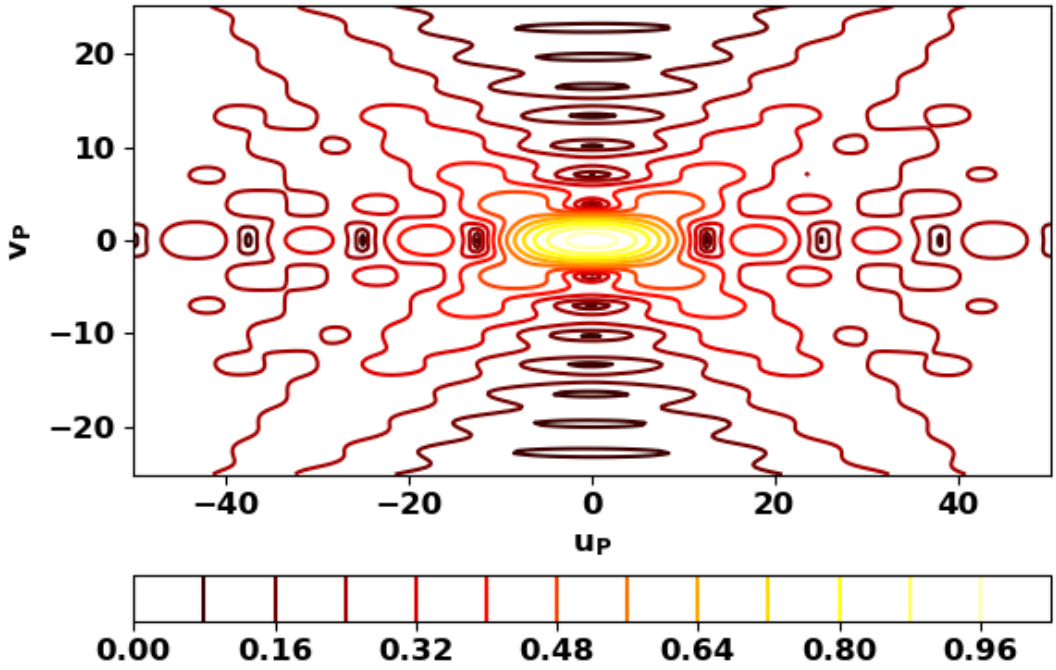

cf = ax.contour(UP,VP,IZX**sf, 12,cmap='hot')

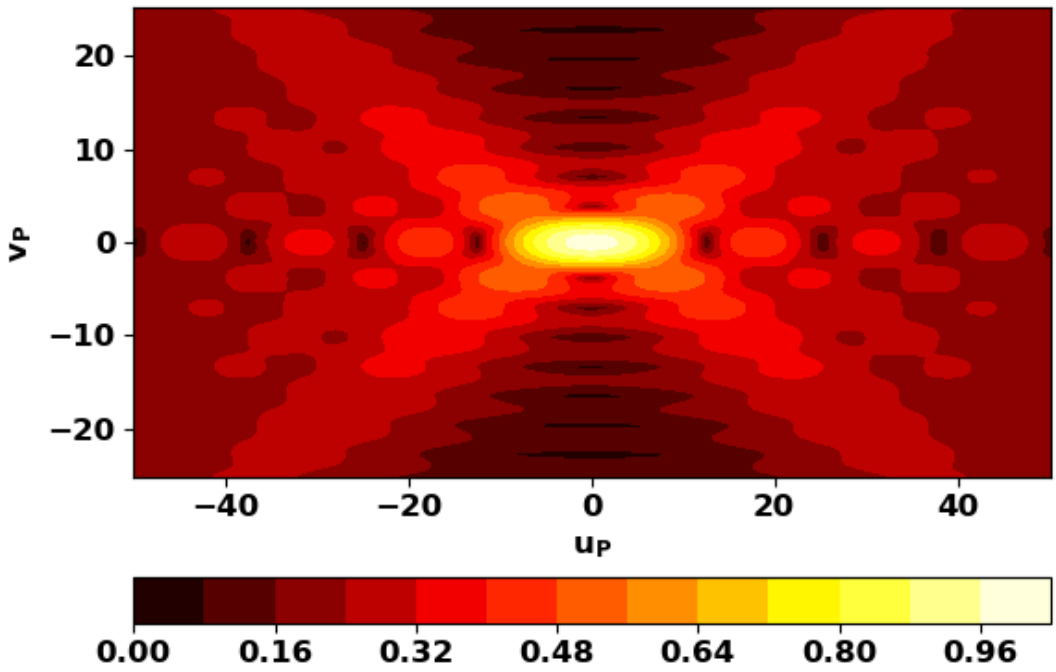

cf = ax.contourf(UP,VP,IZX**sf, 12,cmap='hot')

Fig. 10. [2D] views of the meridional irradiance pattern.

Power contained within circular rings in the focal plane

Fraunhoffer first dark ring vP(dark) = **3.77**
Percentage power within first dark ring Pdark = **85.9**

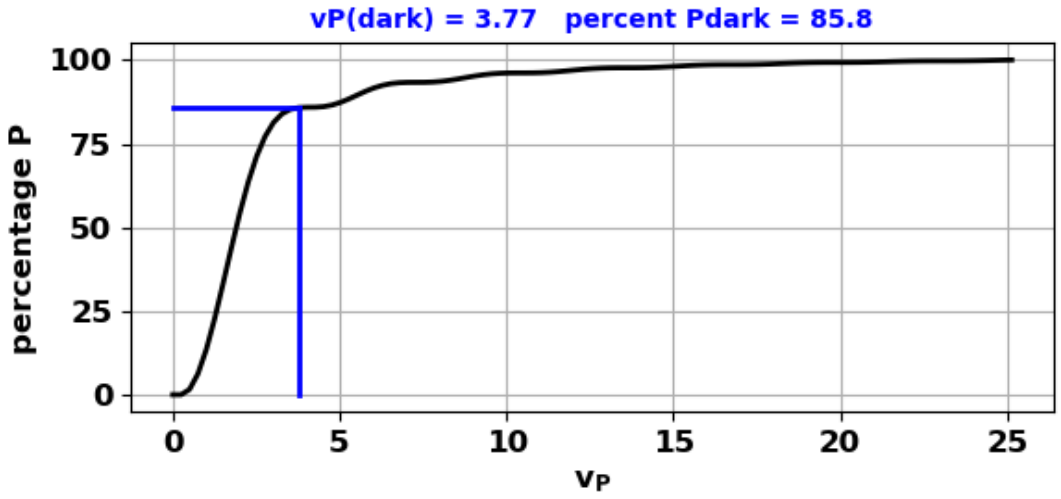

Fig. 11. Focal plane: power contained within circular rings about focal point. 85.8% of the total power is within the first Fraunhoffer dark ring.

Observation XY plane offset from focal plane

$f = z_S$ = 0.020 m z_P = 0.20020 m $offset$ = 0.00020 m

Percentage power within first dark ring Pdark = **49.8**

Graphical results are displayed in figure 12. The power within the radial distance equal to the Fraunhoffer dark ring position (vP_{dark} = 3.77) is only 49.8% composed with 85.8% for the focal plane.

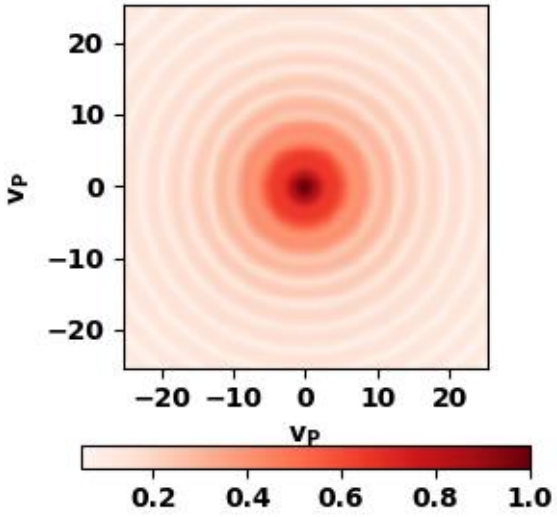
20
10
0
−10
−20
vP
−20 −10 0 10 20
vP
0.2 0.4 0.6 0.8 1.0

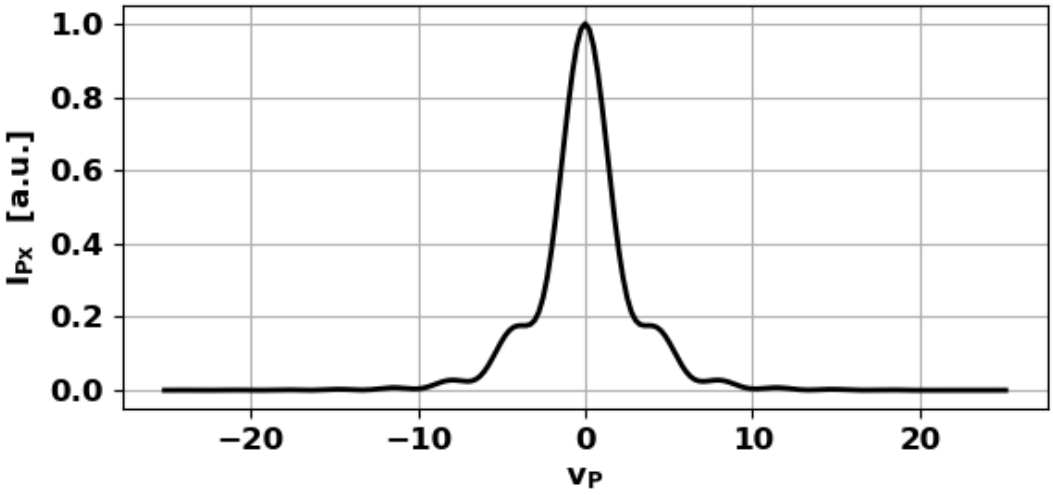
1.0
0.8
0.6
0.4
0.2
0.0
IPx [a.u.]
−20 −10 0 10 20
vP

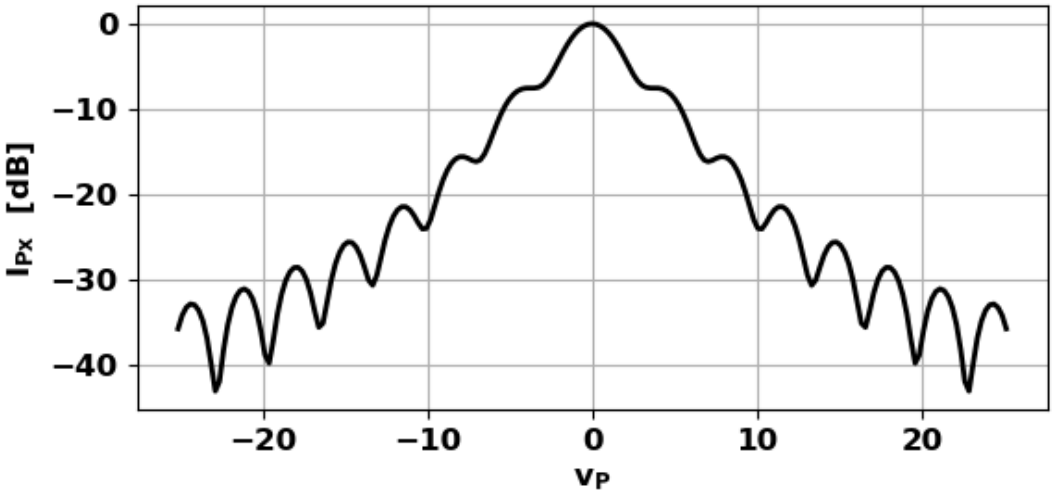
0
−10
−20
−30
−40
IPx [dB]
−20 −10 0 10 20
vP

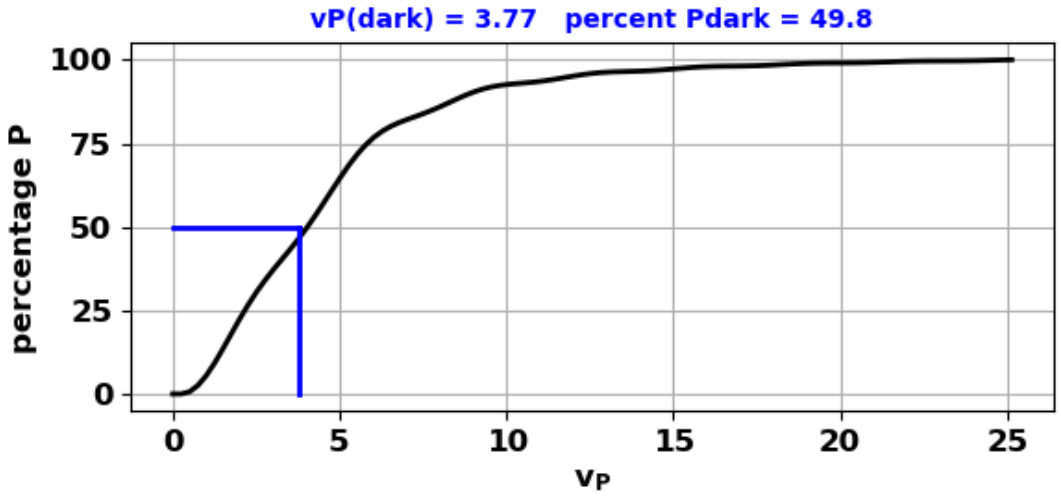

Fig. 12. Graphical results for the observation XY plane offset from the focal plane by 0.20 mm. The power concentration in the focal region (within the Fraunhoffer first dark ring $v_{Pdark} = 3.77$) is reduced from 85.5% to 49.8%.

2. Large NA and large NF

focal length f = 0.020 m aperture radius a = 0.010 m

NA = 0.447 NF = 10000

Source (0,0, **$zP = f$ = 0.020 m**)

Aperture space

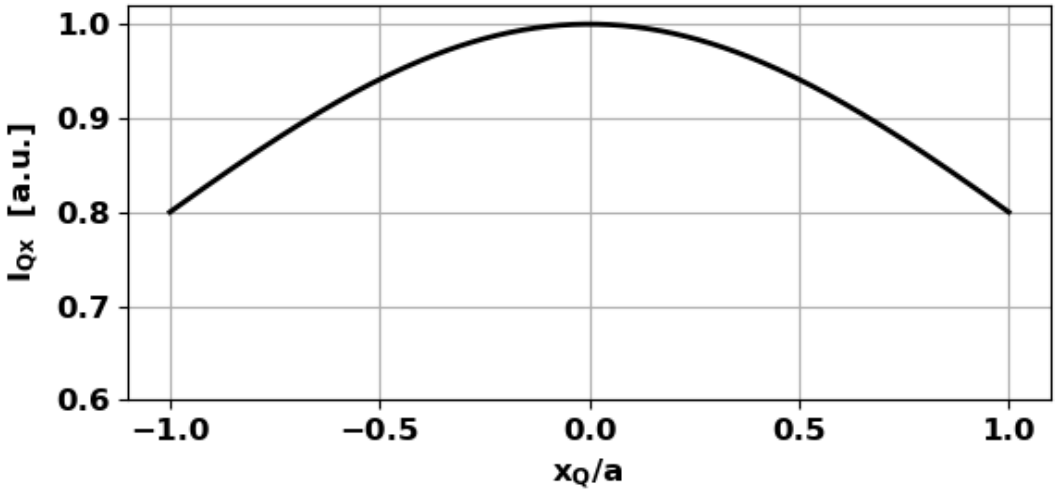

Fig. 13. Aperture space: normalized irradiance distribution along X axis in the plane of the aperture.
$\left(a = 0.010\ \text{m} \quad z_S = 0.020\ \text{m} \quad NQ = 100\right)$

For large values of NA and NF, the Debye – Fraunhoffer approximations are **not** valid.

Observation space

Irradiance along the optical axis near the focal point

emRSFBZ.py

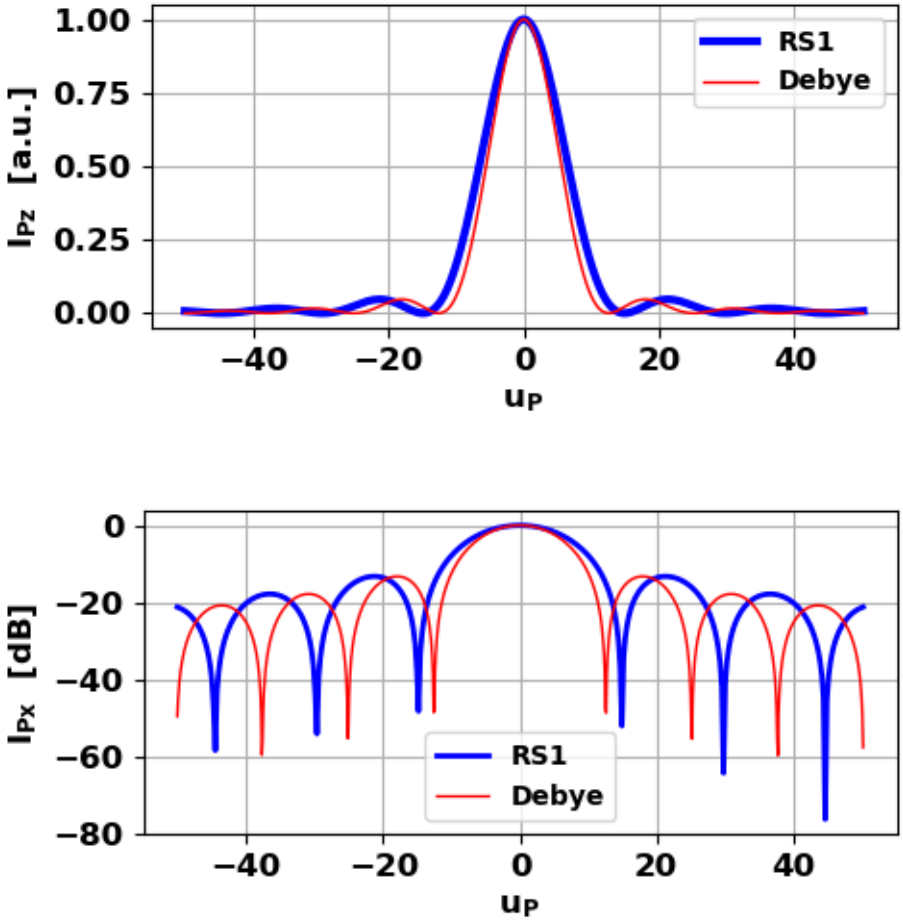

Fig. 14. Normalized irradiance along the optical axis. Blue curve (RS1) and red curve (Debye). For large NA and large NF, the irradiance patterns computed by RS1 and the Debye approximation are very different.

Irradiance in the XY focal plane emRSFBXY.py

Figure 15 shows the dramatic difference between the predictions of the **RS1** calculation and the Debye approximation (equation 12).

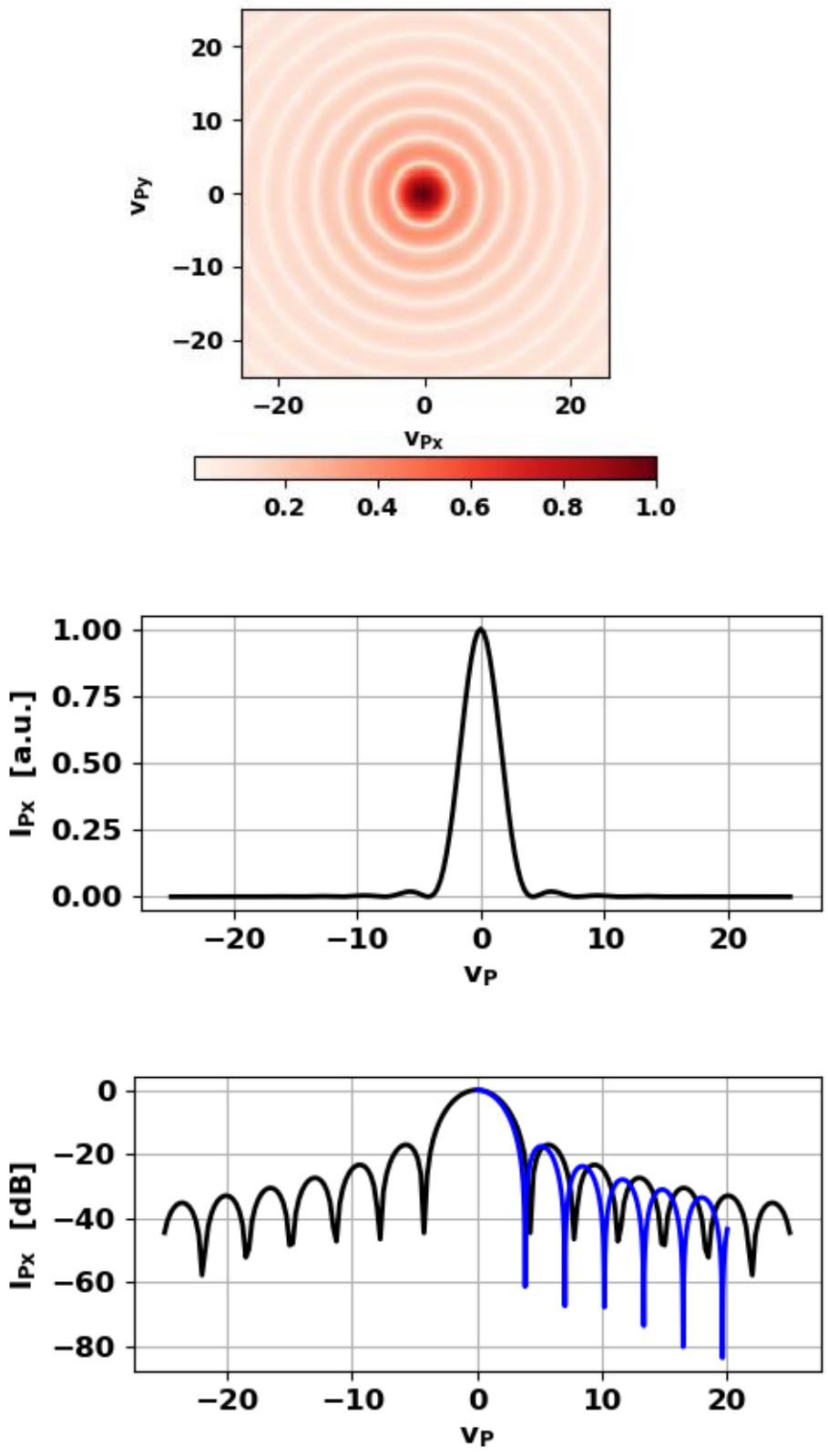

Fig. 15. Normalized irradiance in the focal plane. Blue curve for the Debye approximation

$\left(NP = 120 \quad z_P = 0.020\ m \quad sf = 0.25 \quad I^{sf} \right)$.

The Console Window displays radial coordinate values for the minima in the irradiance distribution for the RS1 and Debye predictions.

Irradiance in the meridional ZX plane emRSFBZX.py

Figure 16 shows the irradiance distribution in the meridional ZX plane.

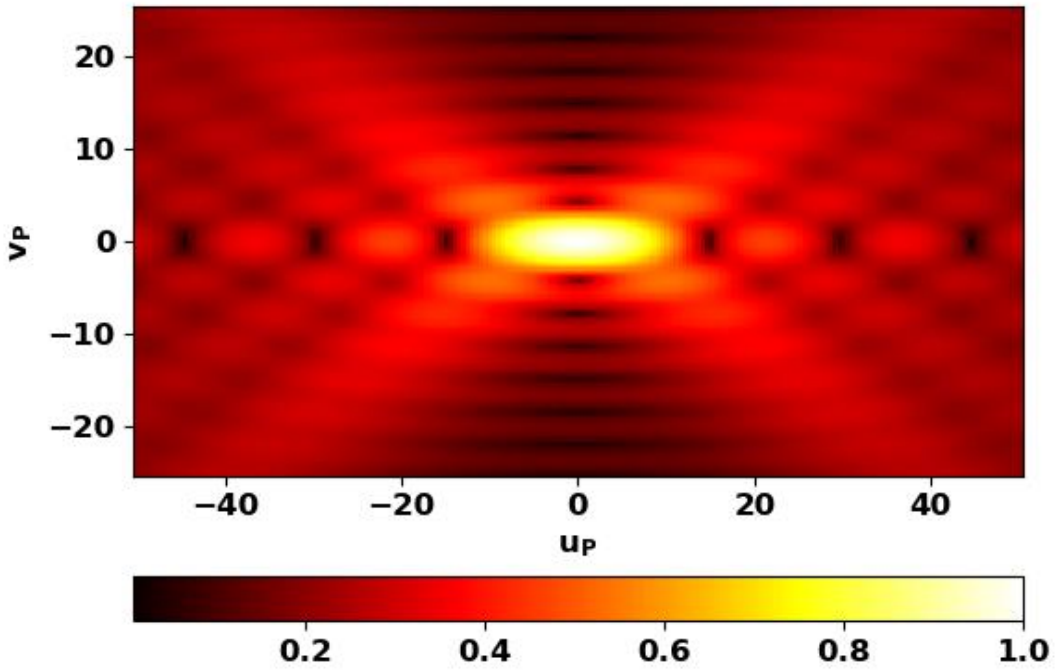

Fig. 16. The irradiance distribution in the meridional ZX plane.

3. Large NA and small NF

focal length f = 0.20 m aperture radius $a = 7.00 \times 10^{-4}$ m

NA = 0.447 NF = 1000

Source (0,0, $zP = f$ = 0.20)

Aperture space

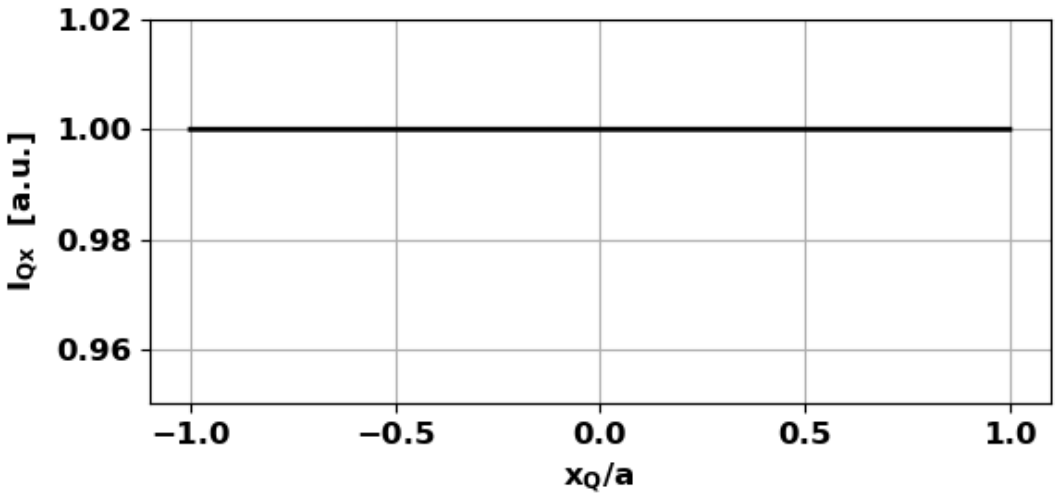

Fig. 17. Aperture normalized irradiance distribution along the X axis.

Observation space

Irradiance along the optical axis near the focal point

emRSFBZ.py

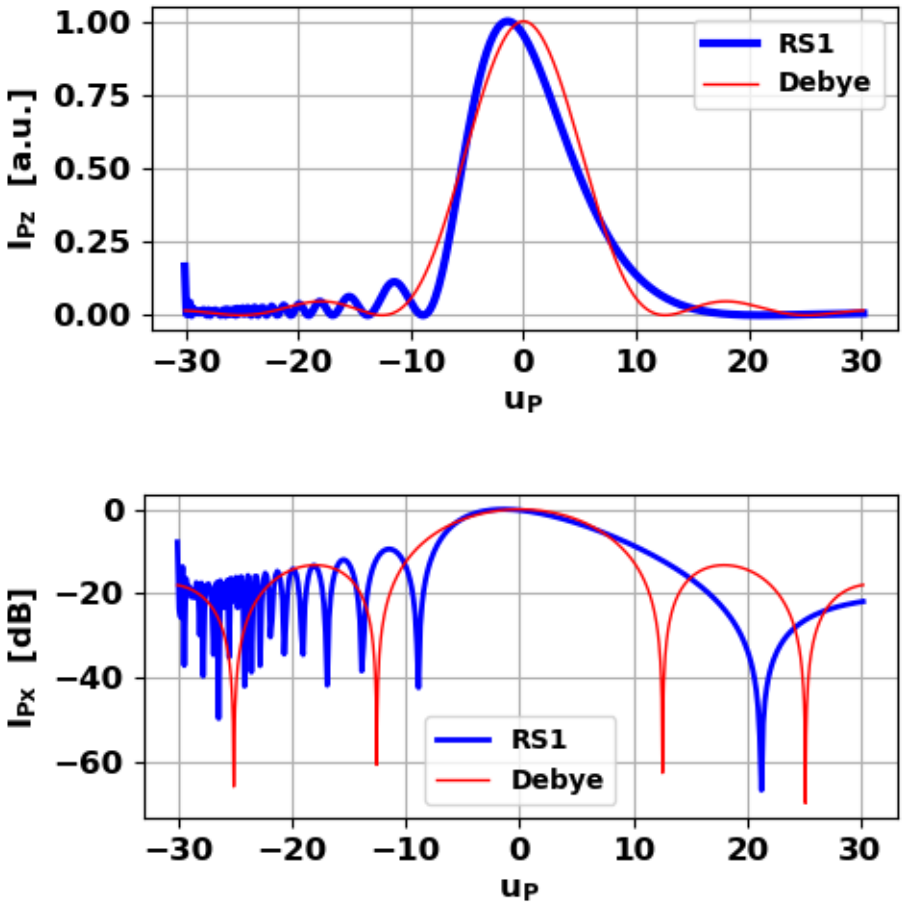

Fig. 18. Irradiance in the axial direction near the focal point. The irradiance pattern is not described by equation 11 (Debye approximation). Note the irradiance pattern is not symmetrical about u_P = 0. **The maximum in the irradiance occurs not at the focus but nearer the aperture**.

Irradiance in the XY focal plane emRSFBXY.py3

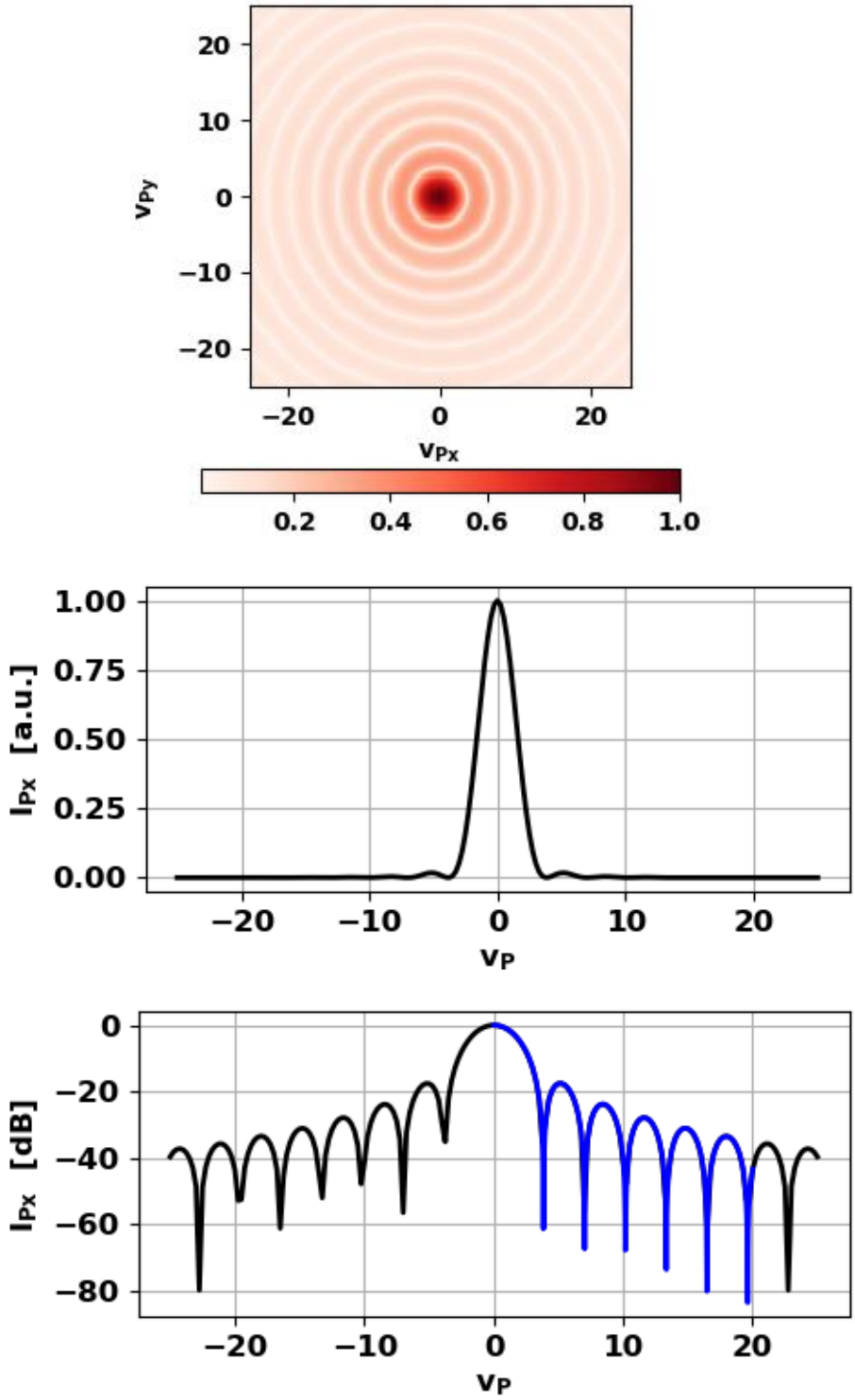

Fig. 19. Normalized irradiance in the focal plane. Blue curve for the Debye approximation. In the radial direction the irradiance can be described by a Fraunhoffer diffraction pattern.

Power contained within circular rings

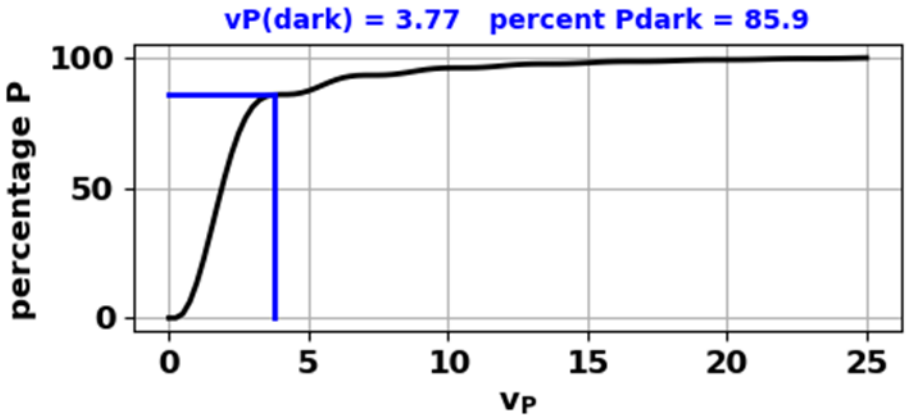

Fig. 20. Focal plane: power contained within circular rings about focal point. 85.9% of the total power is within the first Fraunhoffer dark ring.

Irradiance in the meridional ZX plane emRSFBZX

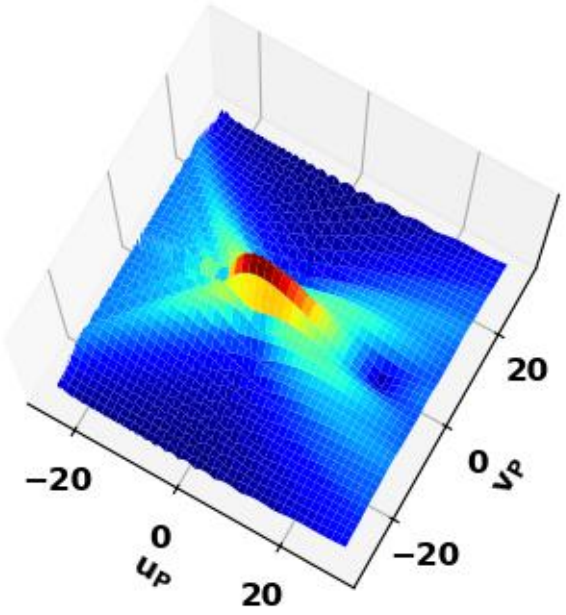

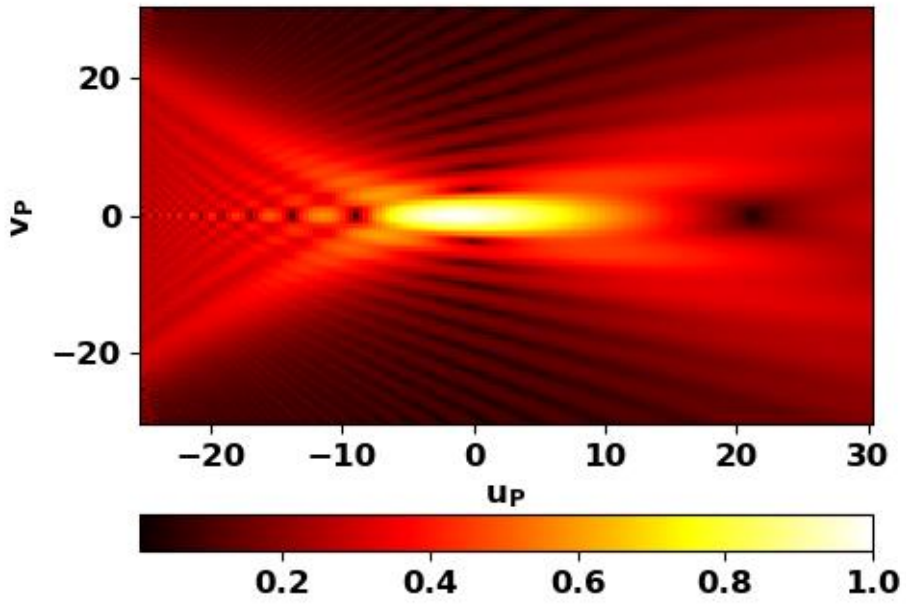

cf = ax.pcolormesh(UP,VP,IZX**sf, cmap='hot')

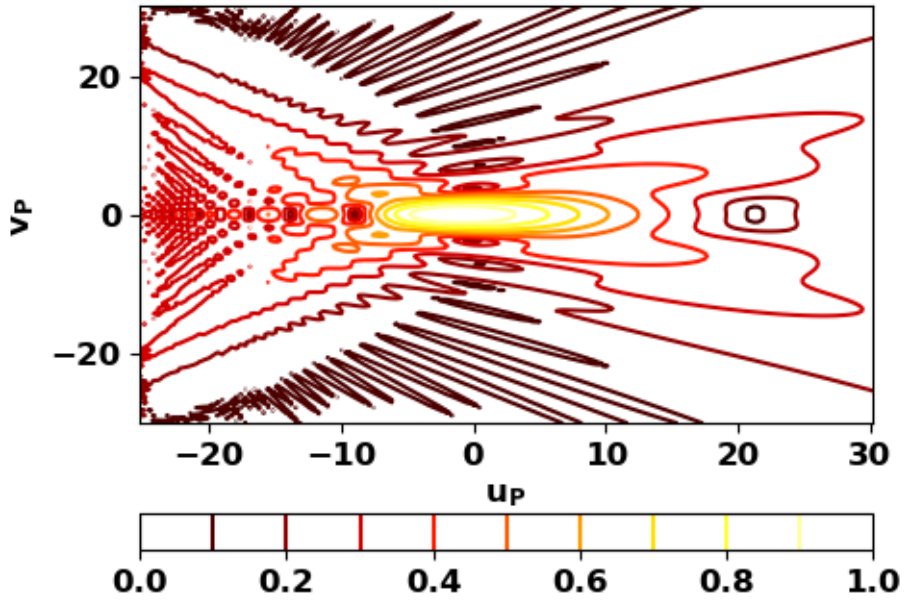

cf = ax.contour(UP,VP,IZX**sf, 12,cmap='hot')

Fig. 21. Irradiance in the meridional ZX plane.